DOI 10.1007/s11237-016-9440-3
Theoretical and Experimental Chemistry, Vol. 51, No. 6, January, 2016 (Russian Original Vol. 51, No. 6, November-December, 2015)

EFFECT OF MECHANOCHEMICAL TREATMENT ON ACIDIC AND CATALYTIC PROPERTIES OF $MgO\text{-}SiO_2$ COMPOSITION IN THE CONVERSION OF ETHANOL TO 1,3-BUTADIENE

O. V. Larina,[1] P. I. Kyriienko,[1] V. V. Trachevskii,[2] N. V. Vlasenko,[1] and S. O. Soloviev[1]

UDC 544.478.1

It was shown that mechanochemical treatment of the $MgO\text{-}SiO_2$ composition leads to an increase of its activity and selectivity in the heterogeneous catalytic conversion of ethanol into 1,3-butadiene. This results from the formation of active reaction sites for aldol–crotonic condensation on the surface of the —Mg—O—Si≡ structural fragments, which are Lewis acidic sites.

***Key words**: $MgO\text{-}SiO_2$, mechanochemical treatment, Lewis acidic sites (LAS), ethanol, 1,3-butadiene.*

The creation of new chemical technologies based on renewable raw materials such as bioethanol and the improvement of existing technologies are priority issues for "green chemistry" research [1]. One such process that has become consistently more relevant in recent years is the synthesis of 1,3-butadiene (BD) (a monomer used in the production of a series of elastomers) by the Lebedev method:

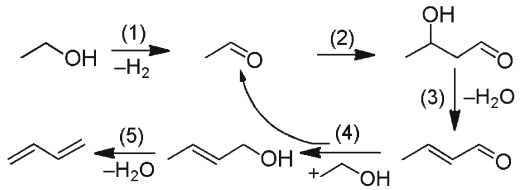

The catalysts used for the conversion of ethanol into BD are metal–oxide compositions combining redox and acid–base characteristics, and this is important for realization of the process [2, 3]. Compositions based on magnesium and silicon oxides doped with compounds of *d* metals (Zn, Ag, Cu) can be used as catalysts for this process [4-8]. The most important way to improve these catalysts is to increase the selectivity of formation of BD and the stability of the operation [9].

[1]L. V. Pisarzhevskii Institute of Physical Chemistry, National Academy of Sciences of Ukraine, Prospekt Nauky, 31, Kyiv 03028, Ukraine. E-mail: olga.larina@ukr.net.
[2]Technical Center, National Academy of Sciences of Ukraine, Vul. Pokrovs'ka, 13, Kyiv 04070, Ukraine. E-mail: trachev@imp.kiev.ua.

Translated from Teoreticheskaya i Éksperimental'naya Khimiya, Vol. 51, No. 6, pp. 378-384, November-December, 2015. Original article submitted October 22, 2015.

The aldol–crotonic condensation of acetaldehyde (AA) [step (2)] is controlling for the catalysts described above and takes place most effectively at the Lewis acidic sites (LASs) on the surface. The active sites of the catalysts, which have basic characteristics, accelerate the aldol condensation with the preferential formation of 1-butanol or ethyl acetate [10]. The important role of the LASs, including the magnesium and silicon oxide phases formed by the —Mg—O—Si≡ fragments in the contact zone [13], for the attainment of high selectivity with respect to BD has been pointed out in a number of papers [11, 12]. One method of intensifying the interaction between the above-mentioned oxides may be mechanochemical treatment [14]. The present work was therefore devoted to study of the effect of mechanochemical treatment of the $MgO\text{-}SiO_2$ composition on its acidic characteristics, activity, and selectivity in the formation of 1,3-butadiene from ethanol.

EXPERIMENTAL

To prepare the catalysts we used a mixture of magnesium oxide ("pure", $S_{sp} = 118$ m^2/g) and silicon oxide (industrial KSKG, treated with nitric acid and calcined at 500 °C, $S_{sp} = 283$ m^2/g) in the ratio $MgO : SiO_2 = 1 : 1$. The sample designated as $MgO\text{-}SiO_2$(WK) was prepared by wet-kneading the initial oxides, and the sample $MgO\text{-}SiO_2$(MC) was produced by mechanochemical treatment in a Fritsch Pulverisette 6 planetary ball mill. Mechanochemical treatment was carried out with silicon nitride balls 20-mm in diameter at 500 rpm (4 h), and the ratio of the mass of the sample to the mass of the balls was 1 : 20. The obtained samples were dried and calcined at 500 °C (3 h).

The X-ray diffraction was performed on a Bruker AXS GmbH D8 ADVANCE instrument in monochromatized CuK_α radiation (nickel filter, $\lambda = 0.154$ nm).

The NMR spectra were recorded on a Bruker Avance 400 spectrometer at 24.494 MHz (^{25}Mg) and 79.495 MHz (^{29}Si) with single- and multi-pulse sequences in the accumulation mode. The chemical shifts (δ, ppm) were determined with reference to the signals of tetramethylsilane (^{29}Si) and a 1 M solution of $Mg(NO_3)_2$ in D_2O (^{25}Mg).

The IR spectra were recorded on a Perkin Elmer Spectrum One Fourier IR spectrometer with a spectral resolution of 2 cm^{-1}. The spectra of the samples (tablets with density of 15 mg/cm^2) were recorded in the region corresponding to the absorption of the hydroxyl groups (3400-4000 cm^{-1}) after preliminary heat treatment at 400 °C for 1 h under vacuum (10^{-3} mm Hg).

The acidic characteristics of the surface of the catalysts were studied by IR spectroscopy with pyridine as molecular probe [8, 13] and by quasi-equilibrium thermal desorption (QE-TD) of ammonia with stepwise increase of temperature [15]. The heat of adsorption of ammonia was calculated by means of the formula proposed in [16].

The specific surface area of the samples was determined by a chromatographic method by thermal desorption of nitrogen on a GKh-1 instrument, with a gas mixture containing 5 vol.% of N_2 in helium.

The catalytic investigations were carried out in a flow-type quartz reactor at 375-400 °C (sample weight 0.5 g). The weight hourly space velocity of ethanol was $W = 1\ g_{EtOH} \cdot g_{cat}^{-1} \cdot h^{-1}$. The experimental procedure and the analysis of the reaction products were described in [8, 13].

The catalytic activity was estimated from the degree of conversion of ethanol (X, %):

$$X = \frac{n^0_{EtOH} - n_{EtOH}}{n^0_{EtOH}} \cdot 100$$

where n^0_{EtOH} is the number of moles of ethanol delivered to the reactor; n_{EtOH} is the number of moles of ethanol in the flow from outlet of the reactor.

$$n = CF$$

where C is the molar concentration of the component in the flow, mol/L; F is the rate of flow, L/h. The selectivity for the carbon-containing products (S, %) was calculated by means of the equation

$$S_i = \frac{n_i}{\sum n_i - n_{\text{EtOH}}} \cdot 100$$

where n_i is the number of moles of the carbon-containing product i in the flow after the reactor.

The material balance in carbon was calculated as the ratio of the total number of moles of carbon-containing products to the total number of moles of ethanol in the initial reaction mixture (not less than 95% calculated on C_1).

The rates of conversion of ethanol (r_{EtOH}, mol/s·m^2) and formation of BD (r_{BD}, mol/s·m^2) were calculated by means of the equations

$$r_{\text{EtOH}} = \frac{WX}{S_{\text{sp}} M_{\text{EtOH}} \cdot 3600 \cdot 100},$$

$$r_{\text{BD}} = \frac{r_{\text{EtOH}} S_{\text{BD}} \cdot 0.5}{100}$$

where W is the weight hourly space velocity of the reagent; S_{sp} is the specific surface area of the sample; M_{EtOH} is the molar mass of ethanol, g/mol; 0.5 is a coefficient that takes account of the formation of one molecule of butadiene from two molecules of ethanol.

RESULTS AND DISCUSSION

Physicochemical Characteristics. On the diffractogram of the initial MgO (Fig. 1a, curve 1) there are two reflections (2θ = 36.92°, 42.9°) corresponding to the cubic lattice of magnesium oxide [17] and a reflection (2θ = 38.2°) corresponding to the hexagonal lattice of magnesium hydroxide [18]. The halo in the region of 20°-30° in the diffractogram of the initial SiO_2 (Fig. 1a, curve 2) is due to the presence of the amorphous phase of silicon dioxide.

In the case of the MgO-SiO_2(WK) sample the diffractogram (Fig. 1a, curve 3) contains reflections corresponding to the crystalline magnesium oxide phase, and their intensity in the sample here is lower than for the initial MgO. The decreased crystallinity of the MgO phase may be due to the increased surface imperfection of the magnesium oxide crystals resulting from interaction with the SiO_2 [5] and to the formation of X-ray amorphous magnesium–silicate phases.

On the diffractogram (Fig. 1a, curve 4) of the MgO-SiO_2(MC) sample there are reflections corresponding to the phases both of crystalline magnesium oxide (2θ = 36.92°, 42.9°) and of crystalline magnesium silicates (2θ = 23.3°, 27.0°, 33.6°, 35.95°, and 52.8°) in particular to forsterite [19].

Figure 1b shows the ^{25}Mg NMR spectra of the MgO-SiO_2(WK) and MgO-SiO_2(MC) compositions, which represent the superimposition of two signals: a narrow signal corresponding to magnesium atoms whose coordination sphere can be represented as a polyhedron of high symmetry with the oxygen atoms at the vertices, characteristic of the MgO phase [20]; a broadened signal corresponding to magnesium atoms whose environmental symmetry is significantly reduced, indicating change in their local environment in comparison with the initial state on account of interaction with the SiO_2. For the MgO-SiO_2(MC) sample in the ^{25}Mg NMR spectrum, in addition to the narrow signal (δ_1 = 30 ppm; $\Delta\nu_1$ = 3.1 kHz) of the MgO phase not involved in the interaction, there is a broad signal (δ_2 = 40 ppm; $\Delta\nu_2$ = 106 kHz) for the magnesium atoms; this indicates more extensive transformation of the MgO phase during interaction with the MgO-SiO_2(WK) composition, characterized by the following ^{25}Mg NMR parameters: δ_1 = 10 ppm, $\Delta\nu_1$ = 150 Hz (the narrow signal) and δ_1 = –46 ppm, $\Delta\nu_1$ = 21 kHz (the broad signal).

Comparison of the ^{25}Mg NMR signals of the products from the reaction between MgO and SiO_2 and published data on magnesium silicates [20, 21] gives reason to consider, in the case of the composition produced by the wet-kneading, that the composition and structure of the surface layers of the particles of the reacting substances change while their internal structure is preserved. On account of the larger amount of disordering in the structure of amorphous silicon dioxide it is possible to suppose that structures with complex spatial organization are formed in the contact zone of the oxide phases, resulting in an increased

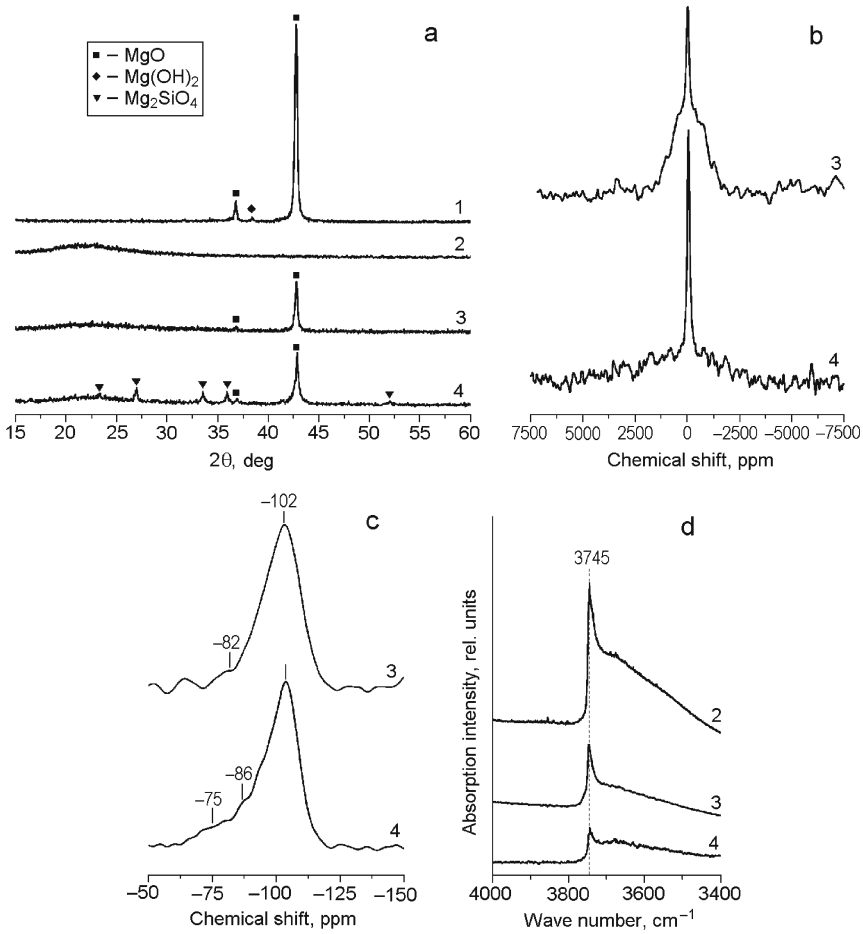

Fig. 1. Diffractograms (a), the ^{25}Mg (b) and ^{29}Si (c) NMR spectra, and the IR spectra in the region corresponding to the absorption of OH groups (d) for the samples of: 1) MgO; 2) SiO_2; 3) MgO-SiO_2(WK); 4) MgO-SiO_2(MC).

degree of screening of the ^{25}Mg nuclei and, as a consequence, an upfield shift of the ^{25}Mg NMR signal in comparison with the position of the signal for the MgO phase not undergoing physicochemical transformation. During interaction between the oxide phases during their mechanochemical treatment defective magnesium–silicate structures are formed [21].

In the ^{29}Si NMR spectra recorded during rotation of the samples by the "magic" angle (Fig. 1c) the signal with δ = –102 ppm, corresponding to four-coordinated silicon atoms $Si(OSi)_3(OH)$ [5], predominates in the observed superimposition, and this is typical of the initial silicon dioxide. The ^{29}Si NMR spectrum of the MgO-SiO_2(WK) sample contains a signal with δ = –82 ppm due to the formation of magnesium–silicate structures $Si(OMg)(OSi)_2(OH)$ [5, 22, 23]. In the ^{29}Si NMR spectrum of the MgO-SiO_2(MC) sample, together with signals with δ = –102 and –86 ppm, there is a signal with δ = –75 ppm that can be assigned to magnesium–silicate structures $Si(OMg)_2(OSi)_2$ [5].

The magnesium ions on the surface of amorphous silicon dioxide are probably fixed by the formation of a surface amorphous magnesium silicate phase, which can be regarded as a layer of amorphous magnesium silicate on the surface of silica [23]. Mechanochemical treatment promotes the formation and local crystallization of layers of magnesium silicate as a result of heating up of the amorphous phase in the contact zone of the reacting oxide phases.

The suggestion about interaction of the hydrated phases of magnesium and silicon oxides in their contact zone is confirmed further by the nature of the IR spectra in the region corresponding to the valence vibrations of the hydroxyl groups (Fig. 1d). The decreased intensity of the band at 3745 cm^{-1}, attributed to the stretching vibrations of isolated hydroxyl groups on the surface of silica gel [24], in the IR spectra of the investigated compositions compared with the initial silicon dioxide

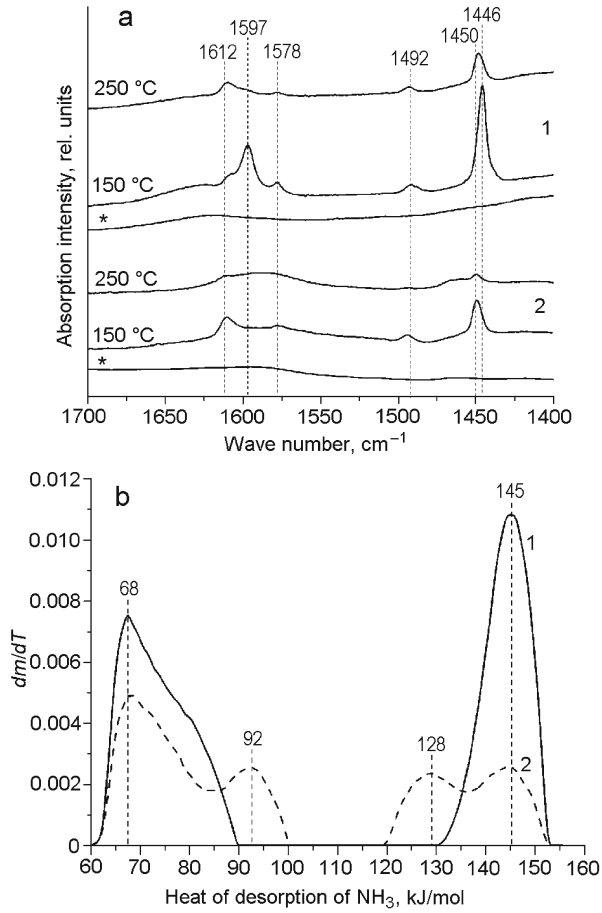

Fig. 2. The IR spectra of adsorbed pyridine after thermal vacuum treatment at the indicated temperatures (a) and differential curves for the temperature variation of mass (*dm*/*dT*) as a result of desorption of ammonia (b): 1) MgO-SiO_2(WK); 2) MgO-SiO_2(MC) (*background spectrum of sample before adsorption of pyridine after heating at 400 °C under vacuum).

indicates condensation of the —Mg—OH and ≡Si—OH groups in their contact zone and the formation of —Mg—O—Si≡ fragments. It should be noted that the intensity of the given band for the MgO-SiO_2(MC) sample is significantly lower than for the MgO-SiO_2(WK) composition.

Acidic Characteristics. In the IR spectra of adsorbed pyridine after thermal treatment at 150 °C under vacuum on the surface of the MgO-SiO_2(WK) sample (Fig. 2a) there are absorption bands attributed to pyridine molecules coordination-bonded with the Lewis acidic sites (1450, 1578, and 1612 cm^{-1}) and pyridinium cations (1446 and 1597 cm^{-1}) and indicating the presence of hydroxyl groups [11]. The low-intensity band (1492 cm^{-1}) can be assigned both to the coordination-bonded pyridine and to the pyridinium ions. In the case of the MgO-SiO_2(MC) sample at a pyridine desorption temperature of 150 °C absorption bands are clearly observed for the pyridine molecules coordination-bonded with the LASs, but at 250 °C they are weaker than those for MgO-SiO_2(WK). At the same time the intensity of the bands corresponding to the pyridinium cations at 150 °C for the sampled obtained by the mechanochemical method is substantially lower than in the case of the sample obtained by the wet-kneading.

Figure 2b shows the profiles of the distribution of acidic sites on the heat of desorption of ammonia, and Table 1 shows the data on concentration of acidic sites and values of adsorption heat of ammonia, characterizing strength of acidic sites. There are weak (60-100 kJ/mol) and strong (120-155 kJ/mol) acidic sites on the surface of the samples. In accordance with the results of IR spectroscopy of adsorbed pyridine and considering the literature data [25] the sites can be referred to the hydroxyl groups

TABLE 1. Characteristics of the Acidic Sites of the Samples According to Data from Quasi-Equilibrium Thermal Desorption of Ammonia

Characteristic	Sites		MgO-SiO_2(WK)	MgO-SiO_2(MC)
Concentration of acidic sites, mmol/g [μmol/m^2]	Weak	w_1	0.43 [2.4]	0.25 [2.5]
		w_2		0.15 [1.5]
	Strong	s_1		0.14 [1.4]
		s_2	0.58 [3.3]	0.15 [1.5]
	Total		1.01 [5.7]	0.69 [6.9]
Heat of adsorption of ammonia, kJ/mol	Weak	w_1	68	68
		w_2		92
	Strong	s_1		128
		s_2	145	145
	Maximum		152	152

TABLE 2. The Effect of Mechanochemical Treatment on the Activity and Selectivity of the Composition Based on Magnesium and Silicon Oxides in the Conversion of Ethanol into 1,3-Butadiene (W = 1 $g_{EtOH} \cdot g_{cat}^{-1} \cdot h^{-1}$)

Catalyst (S_{sp}, m^2/g)	T, °C	Conversion of ethanol, %	Selectivity for products, %				$r_{EtOH} \cdot 10^8$, mol/s·m^2	$r_{BD} \cdot 10^9$, mol/s·m^2
			BD	AA	Ethylene + DEE	Others		
MgO-SiO_2(WK) (176)	375	15.8	33.0	8.8	57.2	1.0	0.54	0.89
	400	31.8	33.4	3.2	60.1	3.3	1.09	1.82
MgO-SiO_2(MC) (100)	375	21.6	48.7	14.9	33.6	2.8	1.30	3.17
	400	41.2	57.3	4.5	34.4	3.8	2.48	7.11

and LAS, respectively. For a sample of MgO-SiO_2(MX) we can observe the appearance of sites with the heat of desorption of ammonia of 92 kJ/mol, which are responsible for hydroxyl groups, and 128 kJ/mol, which correspond to the LASs formed during mechanochemical treatment of the amorphous phase of magnesium silicate. The concentration of strong LASs characterized by the heat of adsorption of ammonia of 145 kJ/mol decreases (Table 1, s_2).

Catalytic Characteristics. The results from investigation of the effect of mechanochemical treatment on the catalytic activity of the composition based on magnesium and silicon oxides in the transformation of ethanol into butadiene are presented in Table 2. From the presented data it is seen that as a result of mechanochemical activation of the mixture of oxides the conversion of ethanol is increased by 1.5 times and at 400 °C reaches 41.2%.

It should be noted that the main products in the presence of MgO-SiO_2(WK) are ethylene and DEE, which are formed as a result of dehydration of ethanol as side reactions. The selectivity of formation of BD for this composition at 400 °C is 33.4%. In the case of the MgO-SiO_2(MC) catalyst the selectivity of formation of ethylene and DEE is lower; the main product is butadiene (selectivity 57.3% at 400 °C). This is probably due to the formation of acidic sites of lower strength and active in the target process

during mechanochemical treatment and to a decrease in the amount of strong LASs that accelerate the dehydration of ethanol. This is confirmed by the data from IR spectroscopy and quasi-equilibrium thermal desorption of ammonia (Fig. 2).

Since a crystalline magnesium silicate phase is formed during mechanochemical treatment of the composition based on magnesium and silicon oxides, the increase in the acetaldehyde content of the reaction products is evidently due also to the stronger redox characteristics of the catalyst surface, which results in a larger yield of BD. The formation of other side products during the conversion of ethanol in the presence of the $MgO\text{-}SiO_2$(MC) catalyst may arise from the participation of acetaldehyde in the aldol condensation processes at the basic centers that are present in the Lewis acid–base pair on the surface of the magnesium oxide by a pathway involving the formation of ethyl acetate and its subsequent transformation into acetone and propylene [9].

In the presence of the sample prepared by the mechanochemical method a significant increase is observed in the transformation rate of ethanol (up to $2.48 \cdot 10^{-8}$ mol/s·m^2 at 400 °C) and in the selectivity of formation of BD. This leads to an increase in the rate of formation of the required product by more than twice (up to $7.11 \cdot 10^{-9}$ mol/s·m^2 at 400 °C). The $MgO\text{-}SiO_2$(MC) sample remains active and selective during repeated working cycles (three cycles in 8 h) with prior regeneration (heating in a stream of 5% O_2 in argon at 500 °C for 2 h).

Thus, the catalytic activity and selectivity in the transformation of ethanol into 1,3-butadiene can be increased by reducing the concentration of strong Lewis acidic sites and forming additional active centers on the surface of the catalyst (LAS of lower strength) with the participation of —Mg—O—Si≡ fragments. In the present work this was achieved by mechanochemical treatment of the $MgO\text{-}SiO_2$ composition.

REFERENCES

1. J. A. Posada, A. D. Patel, A. Roes, et al., *Bioresour. Technol.*, **135**, 490-499 (2013).
2. E. V. Makshina, M. Dusselier, W. Janssens, et al., *Chem. Soc. Rev.*, **43**, 7917-7953 (2014).
3. E. V. Makshina, W. Janssens, B. F. Sels, and P. A. Jacobs, *Catal. Today*, **198**, 338-344 (2012).
4. M. Gao, Z. Liu, M. Zhang, and L. Tong, *Catal. Lett.*, **144**, 2071-2079 (2014).
5. W. Janssens, E. V. Makshina, P. Vanelderen, et al., *ChemSusChem*, **8**, 994-1008 (2015).
6. C. Angelici, M. E. Z. Velthoen, B. M. Weckhuysen, and P. C. A. Bruijnincx, *ChemSusChem*, **7**, 2505-2515 (2014).
7. M. Lewandowski, G. S. Babu, M. Vezzoli, et al., *Catal. Commun*., **49**, 25-28 (2014).
8. O. V. Larina, P. I. Kyriienko, and S. O. Soloviev, *Teor. Éksp. Khim*., **51**, No. 4, 244-249 (2015). [*Theor. Exp. Chem.*, **51**, No. 4, 252-258 (2015) (English translation).]
9. C. Angelici, B. M. Weckhuysen, and P. C. A. Bruijnincx, *ChemSusChem*, **6**, 1595-1614 (2013).
10. A. Chieregato, J. Velasquez Ochoa, C. Bandinelli, et al., *ChemSusChem*, **8**, 377-388 (2015).
11. C. Angelici, M. E. Z. Velthoen, B. M. Weckhuysen, and P. C. A. Bruijnincx, *Catal. Sci. Technol.*, 2869-2879 (2015).
12. M. Zhang, M. Gao, J. Chen, and Y. Yu, *RSC Adv.*, **5**, 25959-25966 (2015).
13. O. V. Larina, P. I. Kyriienko, and S. O. Soloviev, *Catal. Lett.*, **145**, 1162-1168 (2015).
14. J. Temuujin, K. Okada, and K. J. D. MacKenzie, *J. Solid State Chem.*, **138**, 169-177 (1998).
15. N. V. Vlasenko, Y. N. Kochkin, and A. M. Puziy, *J. Mol. Catal. A*, **253**, 192-197 (2006).
16. G. I. Kapustin and T. R. Brueva, *Thermochim. Acta*, **379**, 71-75 (2001).
17. I. M. Abdulmajeed, F. A. Chyad, M. M. Abbas, and H. A. Kareem, *Int. J. Innov. Res. Sci.*, **2**, 5101-5106 (2013).
18. H. Pang, G. Ning, W. Gong, et al., *Chem. Commun.*, **47**, 6317-6319 (2011).
19. F. Tavangarian, R. Emadi, and A. Shafyei, *Powder Technol.*, **198**, 412-416 (2010).
20. K. J. D. MacKenzie and M. E. Smith, *Multinuclear Solid-State Nuclear Magnetic Resonance of Inorganic Materials*, Pergamon Press, Amsterdam (2002).
21. J. M. Griffin, A. J. Berry, and S. E. Ashbrook, *Solid State Nucl. Magn. Reson.*, **40**, 91-99 (2011).
22. J. Temuujin, K. Okada, and K. J. D. MacKenzie, *J. Am. Ceram. Soc.*, **81**, 754-756 (2005).
23. J.-B. d'Espinose de la Caillerie, M. Kermarec, and O. Clause, *J. Phys. Chem.*, **99**, 17273-17281 (1995).
24. S. Haukka, E.-L. Lakomaa, and A. Root, *J. Phys. Chem.*, **97**, 5085-5094 (1993).
25. A. Corma, *Chem. Rev.*, **95**, 559-614 (1995).